DEUTSCHES ELEKTRONEN-SYNCHROTRON DESY

DESY 86-042
April 1986

ELECTRON IDENTIFICATION UP TO 100 GeV BY MEANS OF TRANSITION RADIATION

by

H.-J. Butt, B. Koppitz, S. Nann, R. van Staa
II. Institut für Experimentalphysik, Universität Hamburg

ISSN 0418-9833

NOTKESTRASSE 85 · 2 HAMBURG 52

To be sure that your preprints are promptly included in the
HIGH ENERGY PHYSICS INDEX ,
send them to the following address (if possible by air mail) :

DESY
Bibliothek
Notkestrasse 85
2 Hamburg 52
Germany

DESY 86-042
April 1986

ISSN 0418-9833

Electron Identification up to 100 GeV by means of Transition Radiation

Hans-Jürgen Butt, Bernd Koppitz, Stefan Nann and Rolf van Staa.

2.Institut für Experimentalphysik, Universität Hamburg, Germany

Abstract

We report on measurements with different transition radiation detector configurations, which were performed with the aim of pion-electron-discrimination in the momentum range between 1 GeV c and 100 Gev/c. The test set-up consisted of four polypropylene fibre radiators with proportional wire chambers as photon detectors. We tested about 50 combinations varying the diameter of the fibre, the density of the radiators and the thickness of the chambers. Results of measurements performed at a DESY testbeam at energies between 0.6 and 6.6 GeV and of extrapolations to particle momenta up to 100 GeV/c are discussed. At 95% electron efficiency a pion contamination of a few percent can be achieved over the full energy range.

1 Introduction

Along with the higher energies offered by the next generation of collider facilities the common techniques for particle identification, as Cherenkov counters, time of flight or energy loss measurements, will reach their natural limits. A remaining tool are transition radiation detectors. They may serve for separation of electrons from pions or distinction of hadrons even up to very high energies.

In a previous work [1] we demonstrated that at energies of a few GeV very effective electron-pion-discrimination is achieved with a rather simple detector configuration of four radiator chamber sets, where the radiators consisted of polypropylene fibres. Basing on this experience we investigated how to expand the momentum range of such a

detector up to the order of 100 GeV.

Applied to particle separation, the most important feature of transition radiation is the variation of the yield with the Lorentz factor γ of the incident particle. For an assembly of interfaces - e.g. a stack of foils or an irregular fibre radiator - this behaviour is governed by the plasma frequency ω_P and the material thickness d. According to [2], [3], they can be combined to a parameter $\Gamma = 2.5\,\omega_P[eV]\,d[\mu m]$, which enables one to estimate the γ-dependence of the transition radiation yield obtainable with a foil stack radiator. Being negligible for γ less than 0.5Γ, the yield is increasing rapidly between 1Γ and 2Γ. Beyond 10Γ the radiation energy saturates.

For fibre radiators the picture is more complicated, since the incident particles penetrate layers of strongly varying thickness d. But it still holds that the energy at which pions start to produce remarkable transition radiation (in the following called 'onset energy') can be increased by enlarging the fibre diameter. Therefore with growing diameter, the rejection power of a fibre radiator will become better at high γ-values and worse at low γ-values. To study these correlations was the main topic of our measurements.

To overcome the problem of having no test facility with particle energies as high as necessary two considerations have to be taken into account: Spectra recorded with radiators at the highest available DESY test beam energy (6.6 GeV) are a lower estimate of the yield expected for electrons of higher energies because of the saturation beyond 10Γ. On the other hand, pions of 160 GeV can be simulated by electron measurements at 0.6 GeV. Therefore it is possible to calculate the pion-electron-separation at higher energies without really having a test facility.

2 Experimental arrangements

All measurements were performed at a DESY test beam providing electron energies between 0.6 GeV and 6.6 GeV. The experimental arrangement is sketched in fig.1 and described in detail in [1].

The detector under test was a set up of four radiators with subsequent proportional chamber. The energy deposition was recorded via charge sensitive preamplifiers by peak sensing ADC's of 10 bit resolution. The event trigger, built up by a coincidence of four scintillators, resticted the cross section of the electron beam to less than $1\,cm^2$. A lead glass counter rejected double hit events and electrons with wrong momentum.

As radiators 75 mm long cylinders filled with polypropylene fibres of diameters between 20 μm and 48 μm were tested. The fibres had to be combed with brushes to improve the homogeneity of the density. The self-absorption of photons in the radiator could be reduced by washing the fibres in isopropylalcohol, which removes the surface cladding added for commercial purposes. After those treatments the difference in the yield obtained with fibres of different manufacturers was not very pronounced. Table 1 shows for each diameter the data of the radiator which offered the best results. The density represents a compromise between the number of photons emerging, the mechanical feasibility to keep the fibres compressed and the need for a small overall radiation length. Since the density is nearly equal for all radiators, the average number of layers per radiator length is reduced with increasing diameter.

A radiator of 25 μm polyethylene foils was tested for comparison only, because it will give rise to severe mechanical problems in a large area detector. Foams like 'Etafoam' [8] or 'Rohacell' [9] were excluded during first tests because they could not compete by far. On the other hand, 'Rohacell' seems to be appropriate as bedding material for radiators and chambers.

For the proportional chambers the same design as in our prior tests was applied. But this time we varied the chamber depth between 15 and 30 mm in steps of 5 mm to find the best relation between the contribution of photon absorption and ionization loss.

As filling gas we compared the well proved mixture of Xenon, Argon and Methane (47.5/47.5/5.0) with a new one, where the Argon was replaced by Krypton with respect to the better absorption of high energetic photons beyond the K-shell of Krypton at 14.3 keV. Indeed

the Krypton mixture turned out to be slightly superior, especially for thicker fibres, which made it our final choice. An optimum of chamber depth was found at 25 mm for this mixture.

The chambers were operated at a gas amplification factor of 1600. The resolution was about 25% (fwhm). Calibration was performed by means of the K_α-lines of Copper (8.04 keV) and Silver (22.1 keV). With the help of numerous ionization loss spectra monitored about every two hours during data taking, slight gain variations could be compensated to a negligible degree compared to statistical fluctuations.

3 Data analysis

The effect of transition radiation is demonstrated in fig.2 showing the energy deposition in the first chamber, obtained with the 48 μm fibre radiator at an electron energy of 6.6 GeV. Compared to the Landau distribution there is a clear shift of the radiator spectrum to higher energies. But it is also obvious, that for an effective distinction several pairs of radiator chamber sets are necessary.

The average radiator yield recorded with the 30 μm fibre radiator in the first chamber is plotted versus the electron momentum in fig.3. For comparison the respective curve for the foil stack radiator is added. All data taken with the other fibre radiators show the same shape of energy dependence: After a steep rise the yield flattens or even saturates at a plateau value roughly twice the yield measured for the pure ionization loss (dashed line) . Because of the irregular structur, the plateau obtainable with the fibre radiators, is significantly lower than that of the foil stack.

The data were compared to calculations [1] based on the theory of TR emission of regular foil stacks [2] or randomly spaced fibre radiators [10], [11]. It was assumed that the average fibre diameter is 25% higher than the geometrical one [12], and that the distributions of

[1] The programs were kindly provided to us by Prof.M.Holder, Siegen, and Dr.W. Struczinski, Aachen.

path lengths in material or air are described by Gamma functions. Furthermore the escape effect at the K_α-edge of Krypton and Xenon was assumed to be 22% and 65% respectivly. The result of those calculations (solid line) are in nice agreement with the experimental data.

To determine the pion-electron-separation the likelihood method was applied. Single chamber spectra, as shown for example in fig.1, were smoothed and normalized to unity. They served as distributions of probability that an electron or pion releases a given energy in the chamber. With the products P_e and P_π of the electron and pion probabilties of all chambers a quantity $S = P_e/(P_e + P_\pi)$ was obtained, which is well suited for particle separation.

The probability distribution for pions of 160 GeV (γ = 1200) was derived from data recorded with 0.6 GeV electrons passing through the radiator. In the lower energy range (0.6 GeV - 6.6 GeV), the pion spectrum was simulated by a Landau distribution, which was measured with electrons of 3 GeV and scaled down according to the relativistic rise. The scaling factors, listed in table 2, are derived from different publications ([13],[14],[15]). Finally the distribution of pions at the onset energy is represented by the unscaled ionization loss spectrum.

The probability distributions of electrons at energies available in the test beam were measured directly of course , while the spectra at high energies had to be approximated by the data obtained at 6.6 GeV. This approximation is justified by the saturation behaviour of the radiation yield (fig.3). As a consequence the quoted pion contamination at high energies has to be regarded as an upper limit.

The resulting particle separation properties of e.g. the 30 μm fibre radiator set-up is shown in fig.4a, where the pion contamination is plotted versus the electron efficiency for energies of 2 GeV, 160 GeV and for the onset energy. At the lower energy a very powerful particle separation is achieved although the transition radiation yield is not at its maximum (s. fig.3). It benefits significantly by the smaller ionization loss of pions. At 160 GeV the pions produce transition radiation to a remarkable extent, and consequently the particle separation becomes quite poor. The usefull energy range of a transition radiation detector is limited by the onset energy , where the radiation produced by pions is still negligible. Here the rejection power is worse compared to lower energies, because the increased ionization loss of pions is only partly compensated by the saturated radiation yield.

The onset energy depends on the fibre diameter (s. chapt.1). It can be estimated by the above mentioned calculations, which are well confirmed by our measurements. As onset energy we define the pion energy, at which the average energy deposition observed with a radiator is 2.5% higher than that, of the pure ionization loss. The resulting values are listed in table 3 for the fibre diameters investigated. Although that definition may seem to be somewhat arbitrary, it provides a reasonable estimation of the useful energy range of a given TR detector.

The rejection power can be improved by increasing the number of radiators and chambers. Fig.4b shows for example the pion contamination computed for a set-up of six radiators. In comparison to fig.4a an improvement by a factor of 2 to 6, depending on the energy, can be seen.

The energy dependence of the pion contamination at 95% electron efficiency is plotted in fig.5 for all fibre diameters investigated. In the lower energy range, the rejection power becomes worse with increasing fibre thickness. At the other end of the energy scale this correlation is reversed. Up to the onset energy the pion contamination is not greater than 10% for a detector set-up of four radiators and chambers.

4 Conclusion

Transition radiation detectors with polypropylene fibres provide effective pion-electron-separation at energies even up to the order of 100 GeV. For a given energy range the rejection power can be optimized by carefully adjusting the fibre diameter. For a detector configuration of four radiators and chambers with a total length of 40 cm the pion contamination at 95% electron efficiency is not greater than

10% at energies between 1 GeV and about 100 GeV.

References

[1] A.Büngener et al., Nucl. Instr. and Meth. 214 (1983) 261.

[2] X.Artru, G.B.Yodh, G.Mennessier , Phys.Rev. D 12 (1975) 1289.

[3] J.Cobb et al. , Nucl. Instr. and Meth. 140 (1977) 413.

[4] Hanfspinnerei Steen, 2000 Hamburg 54, Fed. Rep. Germany.

[5] Montedison Deutschland GmbH, 6236 Eschborn, Fed. Rep. Germany.

[6] Neumag Spinnmaschinenfabrik, 2350 Neumünster, Fed. Rep. Germany.

[7] Memminger Folienwerke, 8940 Memmingen, Fed. Rep. Germany.

[8] Dow Chemical, United States.

[9] Röhm GmbH, 6100 Darmstadt, Fed. Rep. Germany.

[10] G.M.Garibian, L.A.Gevorgyan, C.Yang , Zh. Eksp. Teor. Fiz. 66 (1974) 552.

[11] G.M.Garibian, L.A.Gevorgyan, C.Yang, , Nucl. Instr. and Meth. 125 (1975) 133.

[12] M.Baake, diploma thesis (unpublished), Bonn (1984).

[13] J.H.Cobb, W.W.M.Allison, J.N.Bunch, , Nucl. Instr. and Meth. 133 (1976) 315.

[14] A.H.Walenta et al., Nucl. Instr. and Meth. 161 (1979) 45.

[15] W.W.M.Allison, J.H.Cobb, Ann. Rev. Nucl. Part. Sci 30 (1980) 253.

Figure captions

Fig.1 : Schematic view of the experimental arrangement.

Fig.2 : A radiator spectrum (dashed) compared to a Landau distribution (blank) at an electron energy of 6.6 GeV. The radiator spectrum was measured with a 48 μm fibre radiator in front of the first chamber.

Fig.3 : The average energy deposit versus beam momentum for the 30 μm fibre radiator, the 25 μm foil stack and pure ionization loss. The radiator yields are compared to calculations (solid line).

Fig.4 : Pion contamination versus electron efficiency at different particle momenta for a detector set-up of four (a) and six (b) 30 μm fibre radiators with subsequent chamber.

Fig.5 : Pion contamination at 95% electron efficiency as a function of particle momentum for a set-up of four radiators with a subsequent chamber. Values for all fibre diameters investigated are plotted.

diameter (thickness) (μm)	radiator type	radiator length (mm)	radiator density (g/cm^3)	radiation length (%)	number of layers
20	fibre [4]	75	0.14	1.5	484
30	fibre [5]	75	0.14	1.5	323
38	fibre [6]	75	0.15	1.6	268
48	fibre [5]	75	0.16	1.7	223
25	foil [7]	76	0.10	1.1	339

Table 1: Parameters of radiators investigated.

fibre diameter (μm)	onset energy (GeV)
20	62
30	76
38	84
48	92

Table 2: Calculated pion onset energy for the fibre radiators tested.

energy (GeV)	0.6	1.0	2.0	3.0	4.0	5.0	6.6
scaling factor	0.61	0.63	0.69	0.74	0.76	0.78	0.81

Table 3: Ratio of the mean ionization losses of pions and electrons (from refs. 13,14,15).

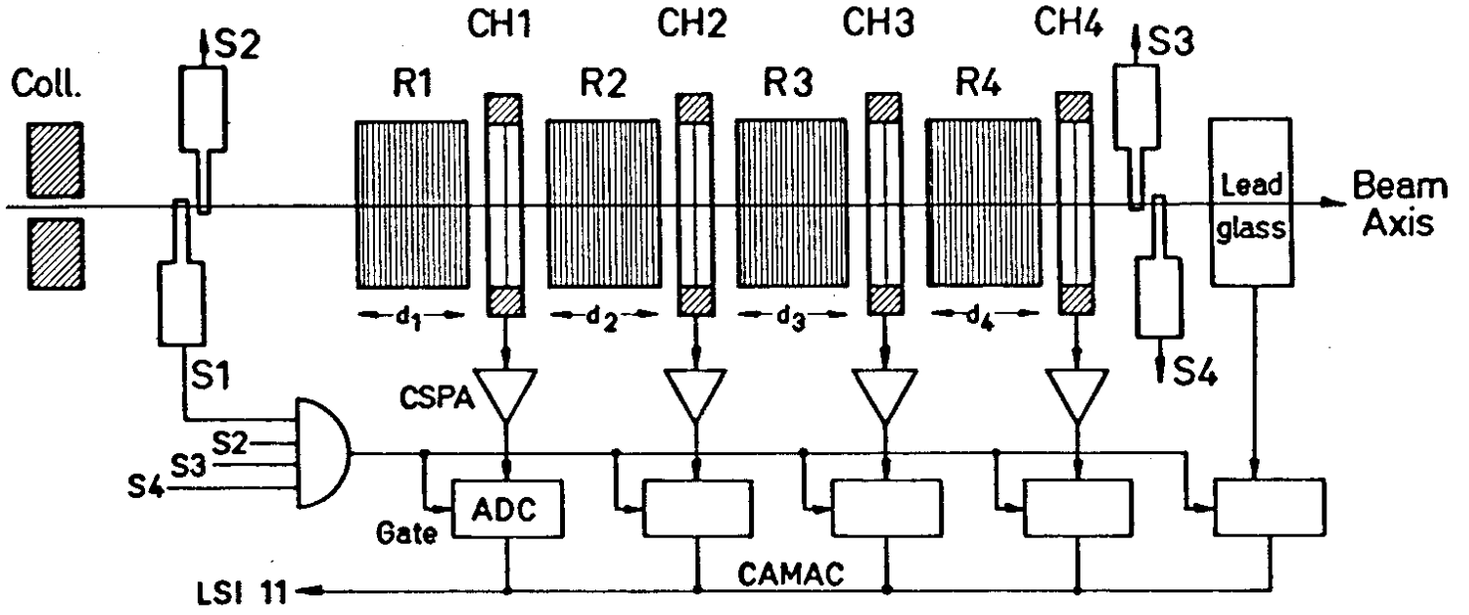
Coll.
S2
CH1
CH2
CH3
CH4
S3
R1
R2
R3
R4
Lead glass
Beam Axis
d_1
d_2
d_3
d_4
S1
S4
CSPA
S2
S3
S4
ADC
Gate
CAMAC
LSI 11

Fig. 1

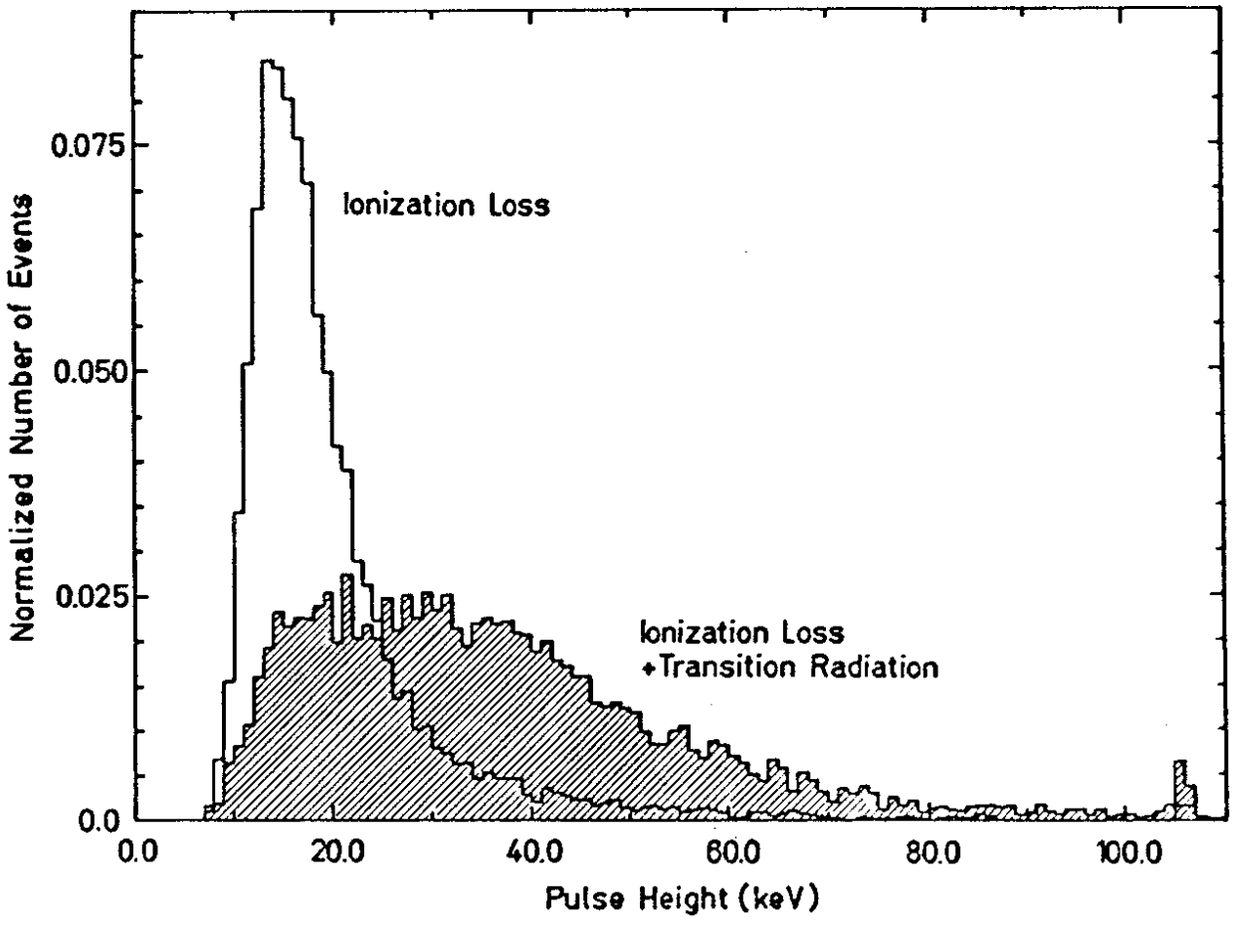
0.075
0.050
0.025
0.0
Normalized Number of Events
Ionization Loss
Ionization Loss
+Transition Radiation
0.0
20.0
40.0
60.0
80.0
100.0
Pulse Height (keV)

Fig. 2

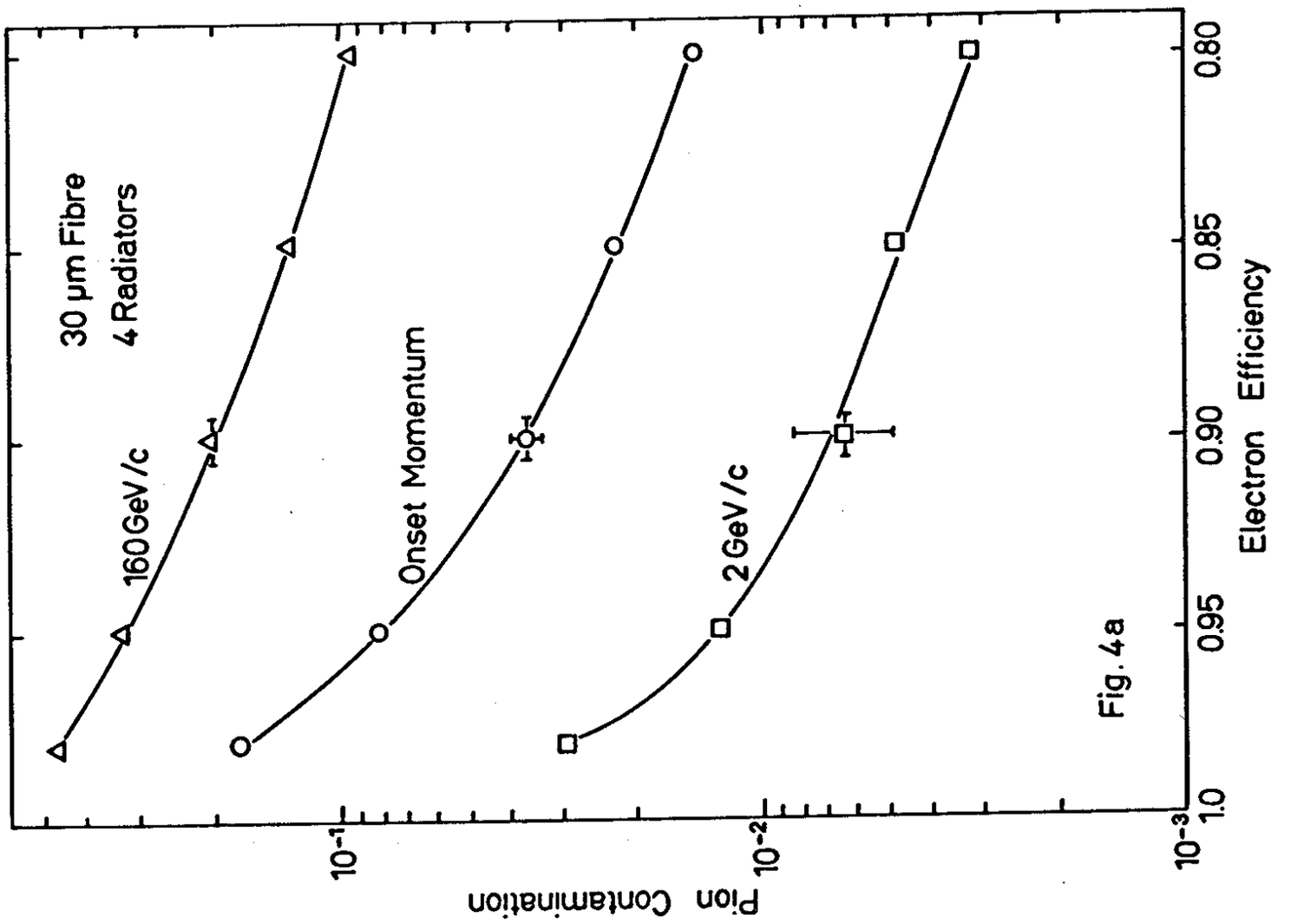
30 µm Fibre
4 Radiators
160 GeV/c
Onset Momentum
2 GeV/c
Pion Contamination
Electron Efficiency
10⁻¹
10⁻²
10⁻³
0.80
0.85
0.90
0.95
1.0

Fig. 4a

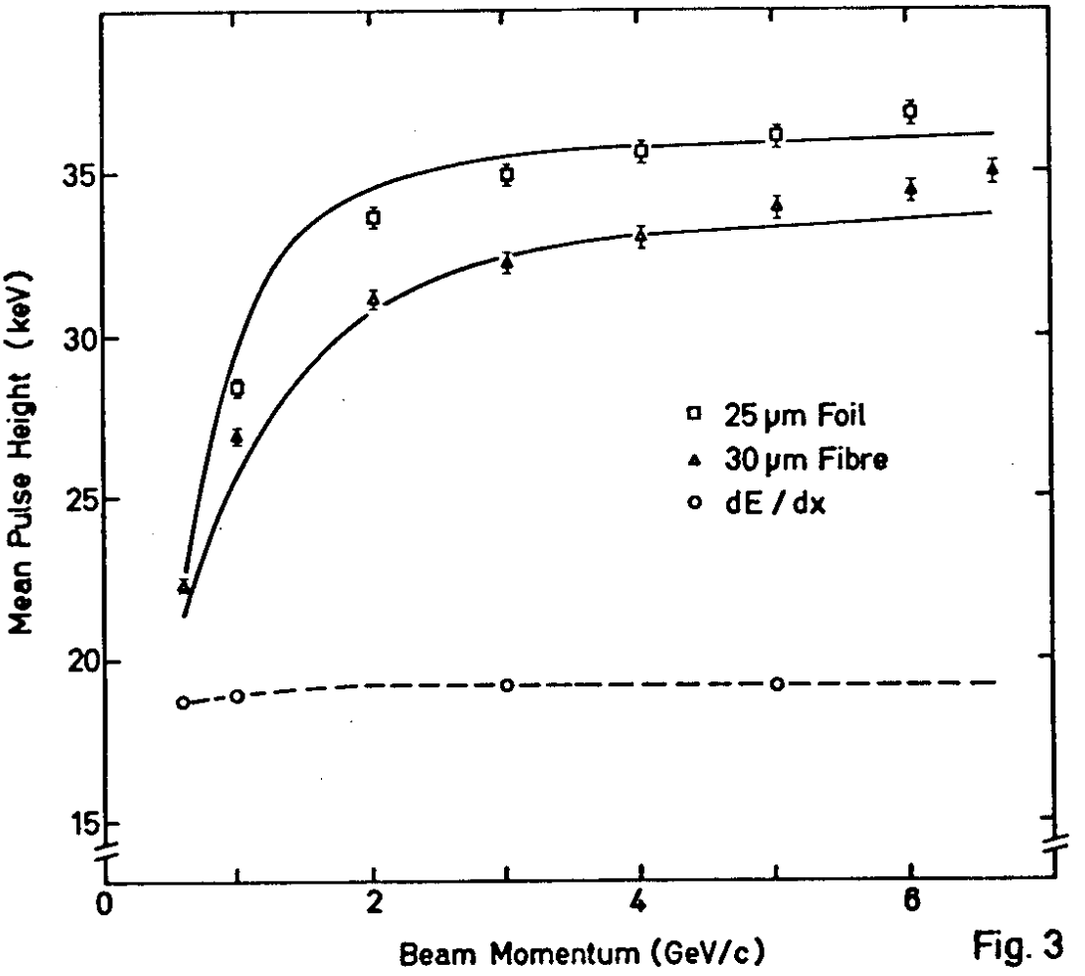
Mean Pulse Height (keV)
Beam Momentum (GeV/c)
25 µm Foil
30 µm Fibre
dE / dx
15
20
25
30
35
0
2
4
6

Fig. 3

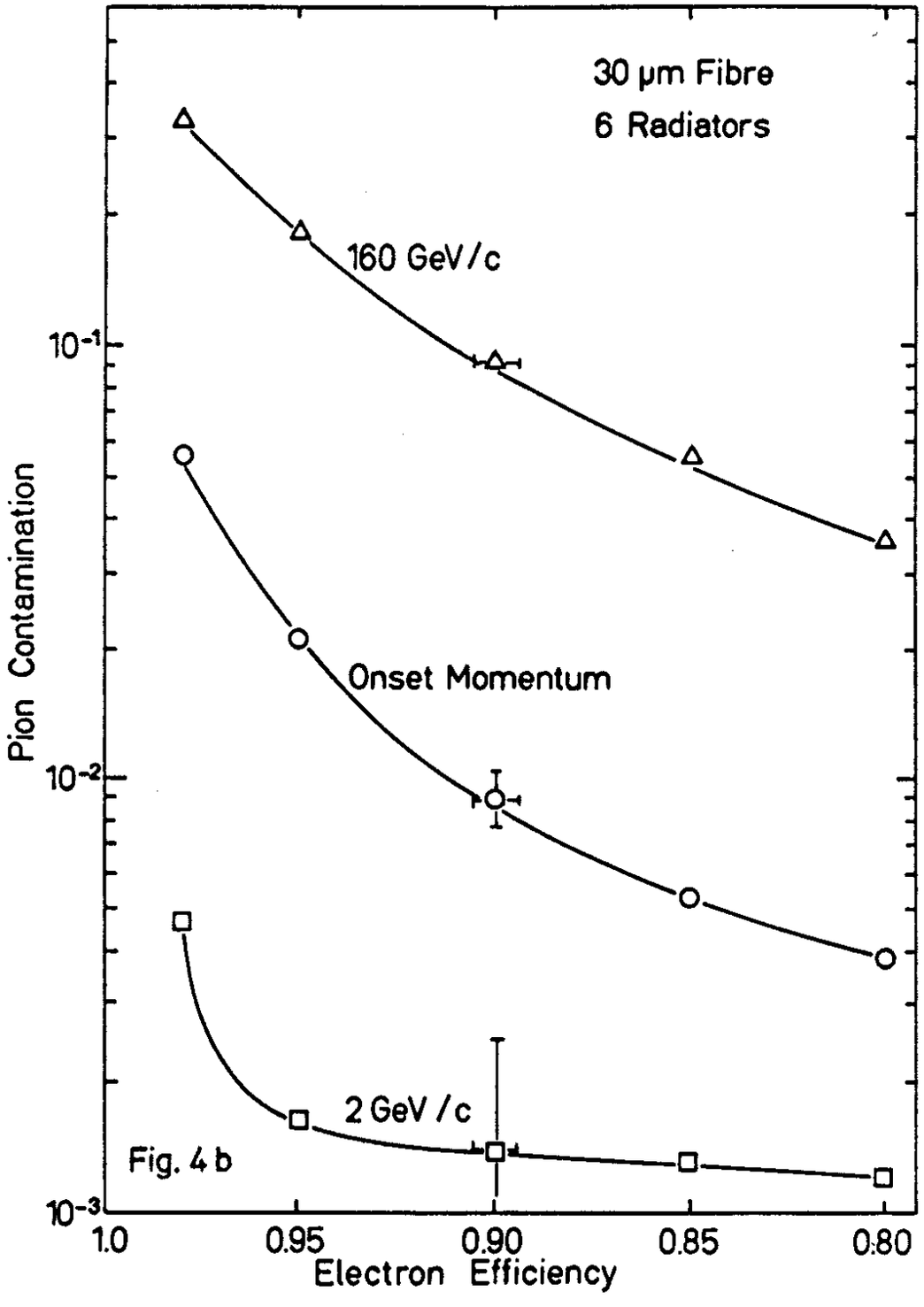
30 μm Fibre
6 Radiators
160 GeV/c
Onset Momentum
2 GeV/c
Pion Contamination
10⁻¹
10⁻²
10⁻³
1.0
0.95
0.90
0.85
0.80
Electron Efficiency

Fig. 4 b

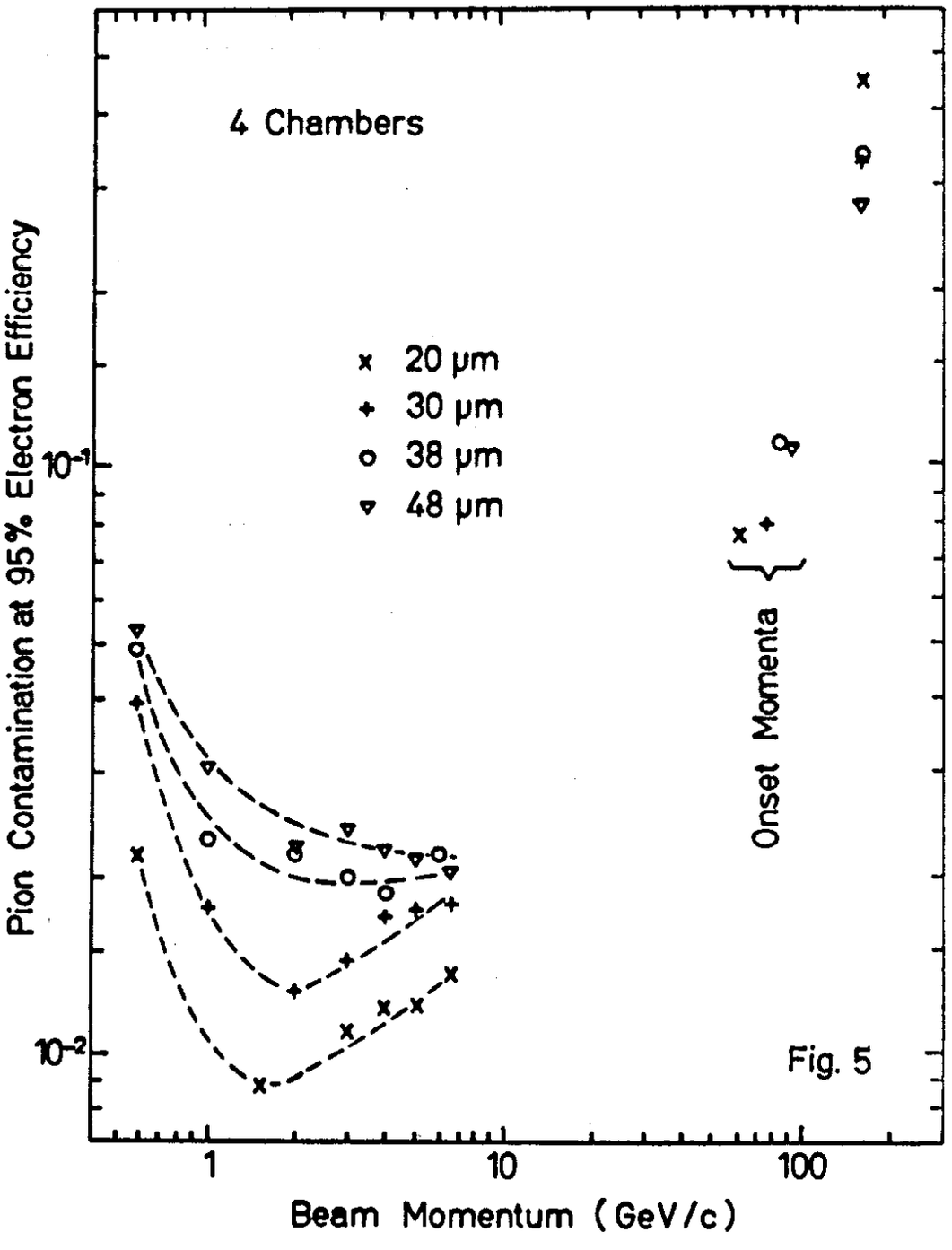
4 Chambers
20 μm
30 μm
38 μm
48 μm
Onset Momenta
Pion Contamination at 95% Electron Efficiency
10⁻¹
10⁻²
1
10
100
Beam Momentum (GeV/c)

Fig. 5